

Health monitoring of a bridge system using strong motion data

K. M. Mosalam*

Department of Civil Engineering, University of California, Berkeley, CA 94720-1710, U.S.A.

Y. Arici

Middle East Technical University, Ankara, Turkey

(Received September 14, 2008, Accepted October 23, 2008)

Abstract. In this paper, the acceptability of system identification results for health monitoring of instrumented bridges is addressed. This is conducted by comparing the confidence intervals of identified modal parameters for a bridge in California, namely Truckee I80/Truckee river bridge, with the change of these parameters caused by several damage scenarios. A challenge to the accuracy of the identified modal parameters involves consequences regarding the damage detection and health monitoring, as some of the identified modal information is essentially not useable for acquiring a reliable damage diagnosis of the bridge system. Use of strong motion data has limitations that should not be ignored. The results and conclusions underline these limitations while presenting the opportunities offered by system identification using strong motion data for better understanding and monitoring the health of bridge systems.

Keywords: concrete bridges; damage modeling; earthquake records; finite element analysis; health monitoring; system identification.

1. Introduction

Health Monitoring (HM) of bridge structures after earthquakes is important for determining the usability of the bridge as well as making repair/replacement decisions. This process is currently performed through visual observation by experienced engineers and is likely to be performed only once a year on a large bridge, e.g. Sylmar I5/14 Interchange Bridge or Truckee I80/Truckee River Bridge (TRB) in California, because of economical and practical limitations. By using online and offline response data, HM of bridge structures is envisioned to be performed remotely with much less effort than visual inspection providing the decision makers with information about the state of the bridge structure after an earthquake.

In the last three decades, considerable research effort was focused on vibration based damage detection techniques. This was mainly motivated by the aerospace industry needs. No attempt is made here to review the vast literature in this area; instead the applications of HM to civil engineering structures excited by earthquakes are briefly reviewed. The application of damage detection to the field of earthquake engineering has not been as prominent as in other fields, due to the relative scarcity of

*Professor and Vice Chair, Corresponding Author, E-mail: mosalam@ce.berkeley.edu

earthquake induced vibration data from instrumented damaged structures. Nevertheless, because of the urgent need to determine the habitability of a structure after a major earthquake, researchers utilized recorded data from recent damaging earthquakes on real structures. Most of these approaches focus on the change of natural frequencies, which are known to decrease after or during strong earthquakes (Beck 1983). However, reduction of frequency is not always due to system damage; such reduction was observed to occur due to environmental conditions (Wood 1992). Large differentials would certainly imply a change in the structural system, but changes to the boundary conditions and soil-structure interaction should not be disregarded (DiPasquale and Cakmak 1990) as these effects are more pronounced for strong motions.

In one of the earliest efforts, a global damage index, strongly related to plastic energy dissipated in the structure during shaking, was used in (Cakmak, *et al.* 1991) to identify damage from earthquake records. The monitoring of the change in modal frequencies was conducted through maximum likelihood estimation with non-overlapping windows. The time variation of the natural frequencies of a building with data from Imperial Valley earthquake using multi-input/multi-output System Identification (SI) method is given in (Mau and Revadigar 1994). SI technique for nonlinear structural systems to estimate time variation of modal parameters and unknown nonlinear behavior is presented in (Loh, *et al.* 1998). On the other hand, a wave propagation approach to damage detection from seismic records is proposed in (Safak 1999). The studies on bridges for damage detection are extensive; mostly utilizing impulse response test results obtained using a controlled input. The work presented in (Farrar and Jauregui 1996) is a good start point for the interested reader to understand the use of experimental modal analysis in HM problem where a well-documented four level damage test was performed on I-40 bridge in New Mexico before its demolishing.

Acceleration recordings from earthquake events are the most common and conveniently used response measurements of bridge structures for obtaining modal property estimates (Arici and Mosalam 2006). Recordings from non-destructive earthquake events can be used for establishing the base-line properties of bridge systems using one of many SI approaches (Arici and Mosalam 2006). Moreover, after damaging earthquakes, strong motion data are readily recorded for many aftershocks that provide vibration data on the damaged state of the bridge. The feasibility of the use of these modal parameters estimates for HM purposes is investigated in this paper using a Finite Element (FE) model for TRB. Sensitivity of the bridge modal parameters to different damage scenarios is determined by manipulating the FE model to simulate damage in the bridge components. The ability to detect these damage cases in the context of the statistical significance of identified healthy modal parameters is assessed. Subsequently, the variation of system modal parameters during a damaging earthquake and aftershocks is evaluated. The use of aftershock recordings for obtaining equivalent linear state-space models of the bridge system is also considered.

2. Objectives and limitations

The main objectives of the work presented in this paper are summarized in the following:

1. Determination of the sensitivity of bridge modal parameters to damage in bridge components;
2. Examination of “detectable” levels of different types of damage on selected bridge components;
3. Assessment of the effect of number of sensors on instrumented bridges for damage detection; and
4. Investigation of the feasibility of using aftershock strong motion data for SI of a damaged bridge.

Notable limitations of the study presented in this paper include the following:

1. Only one bridge structure with widely separated modal frequencies, TRB in Fig. 1a, is investigated.
2. Although a detailed FE model of TRB is used, strength and stiffness degradation and energy dissipation due to damage in concrete bridges is more complex than that adopted in TRB idealization.
3. The statistical significance of the modal parameters estimated from aftershocks is not considered.

3. Sensitivity of modal parameters to damage

The sensitivity of the modal parameters of TRB to changes in system properties are investigated using a pushover analysis of the system. This bridge is a three-span (185', 192', and 185' as shown in Fig. 1a) continuous prestressed concrete with three-cell box-girder deck supported on inverted "A" shaped column bents and constructed in 1989. It was instrumented in 1995 with a total of eight accelerometers as shown in Fig. 1a. The recording of these accelerometers from three small earthquakes that took place in 1998, 2000, and 2001 were studied using different SI techniques (Arici and Mosalam

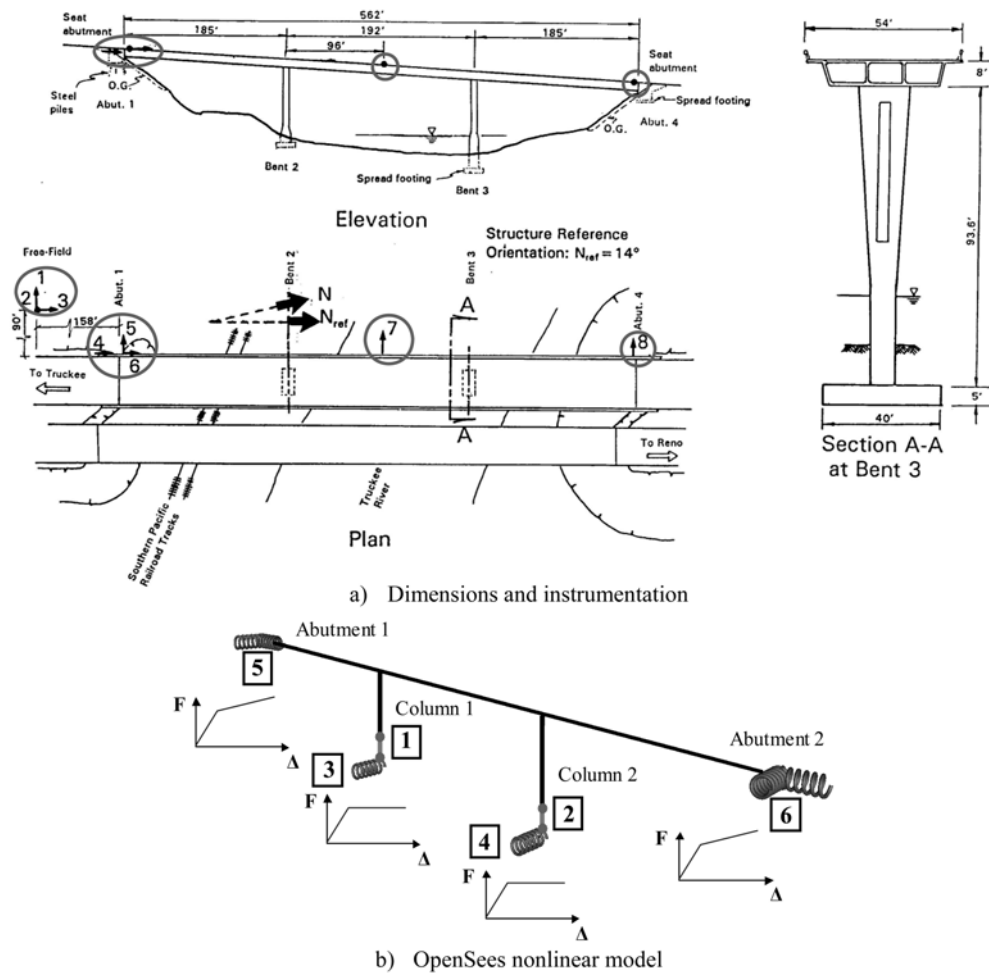


Fig. 1 Truckee-I80/Truckee River Bridge (TRB) and its FE idealization

2003, 2005a, 2005b). The modal frequencies and mode shapes of TRB are evaluated at four critical stages of the pushover analysis. Subsequently, the sensitivity of these modal parameters to column and abutment damages is characterized by varying the FE model.

3.1. OpenSees model for TRB

TRB model, previously simulated using linear analysis in DIANA FE program (De Witte 2003, Arici and Mosalam 2006) is transferred in this study to OpenSees (Open System for Earthquake Engineering Simulation) (Mazzoni, *et al.* 2004) to perform the nonlinear FE analyses presented in this paper. The flexibility offered by OpenSees in terms of nonlinear modeling capabilities and model manipulation led to its selection in the present study as the simulation tool. In this FE model, 16 elastic 2-noded beam elements are used for each span and eight 2-noded beam elements are used for each column. Therefore, the total number of 2-noded beam elements used in this FE model is 64. As shown in Fig. 1b, the bases (bottom elements) of the bridge columns 1 and 2 are modeled using 2-noded beam elements (labeled 1 and 2) based on flexibility formulation to simulate plastic hinging and loss of flexural strength (other elements in the columns are modeled with elastic material). In the transverse direction at the bases of columns 1 and 2, elastic perfectly plastic shear springs (labeled 3 and 4) are provided to account for possible shear failure of the cross-section. The loss of lateral stiffness near the abutments is modeled using shear springs with bilinear properties (labeled 5 and 6) accounting for the displacement and force capacity limits of highway bridges (Maroney and Chai 1994, Goel and Chopra 1995).

The moment-curvature responses, used to model the behavior of the plastic hinge regions at the bases of columns, are determined using fiber section analyses of the cross-sections using the geometry and reinforcement details of the as-built TRB. The concrete material model, used in this analysis, Fig. 2a, utilizes model parameters that are calculated based on the confined concrete material model in (Mander, *et*

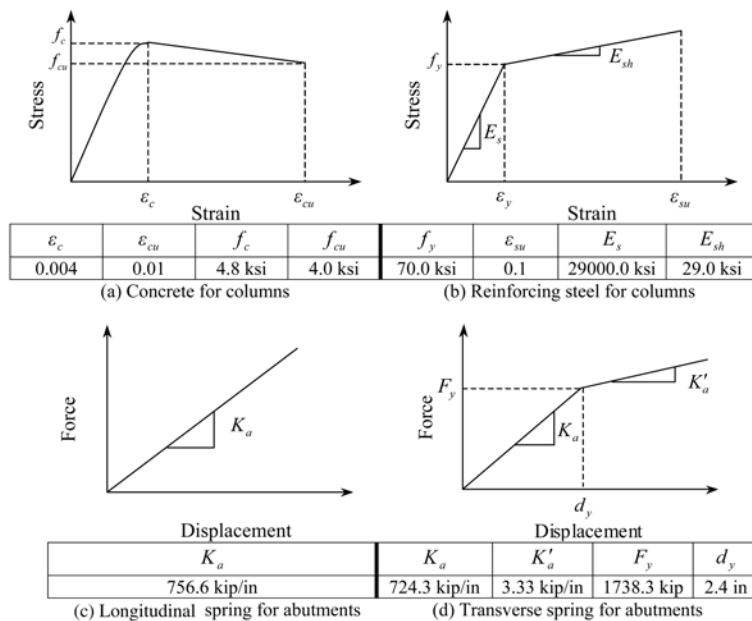


Fig. 2 Constitutive models and parameters used for the TRB elements in the FE model

al. 1988). The constitutive model used for the reinforcing steel, Fig. 2b, is essentially elastic-perfectly plastic as the selected strain hardening is very small. The shear capacity (ACI Committee 318-02 2003) of the columns is based on contributions from concrete, $V_c = 5102$ kip, and transverse steel reinforcement, $V_s = 6473$ kip. Column shear failure is represented by an elastic-perfectly plastic spring at the base with the shear capacity as the failure strength and arbitrarily chosen small displacement at the end of the elastic portion, namely 10^{-6} ft. It is noted that the shear capacity is not critical and does not govern the presented pushover or time history analyses of TRB due to the high shear strength of the bridge columns compared to the shear demands. The abutments are idealized using a bilinear spring in the transverse direction and a linear spring in the longitudinal direction, Fig. 1b. The stiffness parameters for both directions are based on the estimated capacity of the abutments (Arici and Mosalam 2006). The displacement corresponding to change of abutment transverse stiffness is based on (Goel and Chopra 1995). The constitutive models and parameters for these springs are shown in Figs. 2c and d.

3.2. HM based on pushover analysis data

The pushover analysis of TRB is conducted using displacement control, incrementally increasing the displacement of the midpoint of the bridge deck in the transverse direction. The force-displacement response for the bridge is presented in Fig. 3 where four critical stages of the bridge response corresponding to column and abutment failures are marked. These stages correspond to distinct points on the pushover curve where the transverse stiffness of the bridge structure is reduced. The ultimate displacement of the TRB structure is estimated at the flexural failure of both of the bridge columns. As stated before, shear failure of the bases of the columns did not govern the pushover analysis.

For simulation purposes, the DIANA FE model of TRB (Arici and Mosalam 2006) is used to obtain strong motion data for the baseline response (without induced damage) using linear transient analysis with a single input free field ground motion recorded at channel 1 (Fig. 1a) during the 10/30/1998 event (causing small peak recorded deck acceleration at channel 7, Fig. 1a, namely 0.08 g). This linear FE model was validated using the recorded data at channels 1 and 7 (Fig. 1a) by comparison in both time and frequency domains (Arici and Mosalam 2005b). Overall, first and third mode contributions dominated the total response with a relatively weak contribution of the second mode. The transfer function analysis of the output and input data showed negligible contribution of higher transverse modes than the third one. The large structural system of TRB, instrumented on the deck with only three transverse accelerometers, prompted the simulation study using FE analysis to create large number of “sensors” outputs. In that regard, sensors refer to nodal points of the FE model where degrees of freedom are

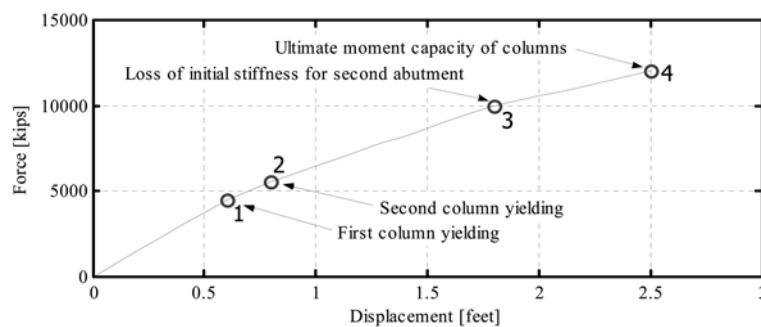


Fig. 3 Force-displacement response and stages of damage of TRB from static pushover FE analysis

Table 1 Configurations of sensors from the FE simulation and levels of noise in data used for TRB

Configuration level	S1	S2	S3	S4	S5	S6
Sensors on deck/columns	3/0	7/0	7/2	13/6	25/14	49/14
Noise level	L1	L2	L3	L4	L4	L5
Standard deviation [% of S6 average standard error]	10	20	25	40	40	50
Standard deviation [%g]	0.09	0.18	0.22	0.36	0.36	0.45

determined from the FE analysis. For investigating the effect of different configurations of sensors on SI results, accelerations from six different sets of the nodal points in the FE model, Table 1, are treated as virtual sensors recordings (Arici and Mosalam 2005b). Moreover, five levels of noise, Table 1, are added to the simulated recordings from the FE analysis creating five different realistic data sets for each configuration of sensors. The added random noise is normally distributed with standard deviation for each noise level selected as percentage of the average of the standard error of the 63 noise-free FE time histories (representing the 63 nodes of the model) from sensor configuration S6. The standard error for each separate time history is calculated by finding the mean of the squared differences between each value and the mean of the time history. It is to be noted that, the recorded data from channel 1, Fig. 1a, is also polluted similarly by adding noise with identical properties to the L1-L5 five levels of random noise to create realistic input time series to the FE simulations for subsequent SI.

In a previous study (Arici and Mosalam 2005b, 2006), the statistical significance of modal parameters identified using strong motion time histories recorded or simulated on TRB was assessed. As an outcome of this study, the confidence intervals of identified modal frequencies and damping ratios were obtained using Monte Carlo simulations and sensitivity analyses in conjunction with Eigen Realization Algorithm (ERA). The dependence of the statistical bounds (in terms of the 95% confidence intervals) on model parameters was examined. Moreover, the effect of using different number of sensors on the statistical significance is evaluated using simulated time history data from the validated FE model of TRB (Arici and Mosalam 2005b) which is also used in this paper with added damage scenarios. The variation of the first modal frequency during the pushover analysis is presented in Fig. 4. This variation is obtained by conducting an eigen solution of the bridge system in OpenSees using the tangent

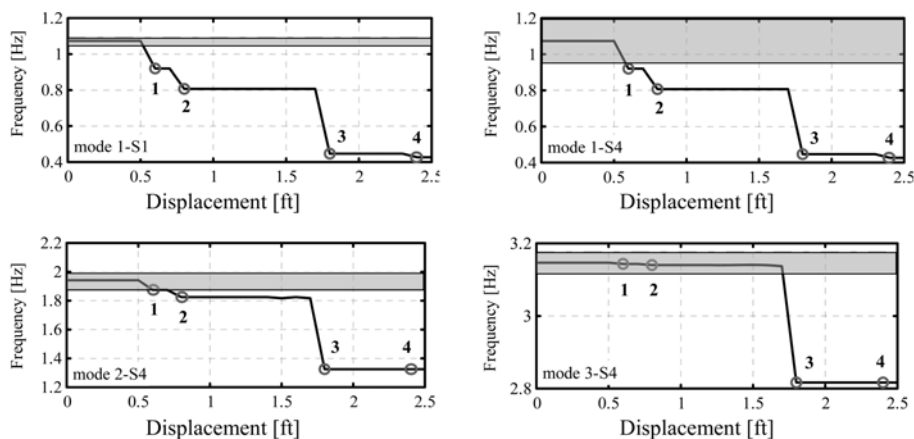


Fig. 4 Variation of the fundamental and higher modal frequencies with TRB deck displacement and confidence intervals for the healthy bridge using data with L5 noise level

stiffness matrix corresponding to the current applied lateral displacement. The 95% confidence intervals (Arici and Mosalam 2005a) for the estimate of the first modal frequency of the healthy system identified from noisy data (noise level L5, Table 1) are also shown in Fig. 4. These intervals are represented by gray bands on the identified fundamental frequency from sensor configurations S1 and S4 (Table 1). For successful damage detection in the system, the change in the modal frequency should exceed the confidence bounds of the healthy modal property. The four stages identified by points in Fig. 3 are also marked on these plots. As observed from Fig. 4, the drastic changes in TRB, i.e. the yielding of bridge columns and the loss of stiffness of abutments, lead to significant changes in the fundamental frequency with variations much larger than the confidence intervals of the identified healthy modal frequency. However, the change in the frequency due to first column yielding could barely be considered statistically significant if the healthy modal property is estimated using S4 sensor configuration where damaged frequency is close to the lower confidence bound of the healthy system in this case of large number of sensors and large noise level (S4 and L5).

The variations of the second and third modal frequencies during the pushover analysis are also presented in Fig. 4. The 95% confidence intervals for the SI estimates of healthy state parameters from noisy data set L5 are provided for sensor configuration S4. As observed, the change in these modal parameters due to the yielding of the first bridge column (and to some extent the second bridge column as well) is not statistically significant when the confidence intervals of estimating these parameters from noisy data are considered. These modal quantities changed remarkably only for the extreme stages of the behavior, i.e. the loss of stiffness for one of the abutments and the ultimate failure of the system corresponding to the flexural strength limit of the bridge columns. The confidence intervals for these higher modal frequencies have not displayed dependencies on sensor configuration (Arici and Mosalam 2005a). Therefore, similar conclusions are valid using SI results with other sensor configurations.

The changes of the mode shapes of TRB are insignificant for stages 1 and 2, i.e. the effect of column yielding on transverse mode shapes of the TRB system is minimal. On the other hand, the mode shapes are significantly affected by the loss of stiffness of the abutment and failure of columns observed in stages 3 and 4, respectively. The variations in the mode shapes are compared to the confidence intervals of the identified healthy mode shapes obtained from (Arici and Mosalam 2005a). For the first mode, the level of noise in the recorded data is observed to be crucial for the determination of whether the change in the mode shape is statistically significant or not. As observed from Fig. 5, for SI conducted using

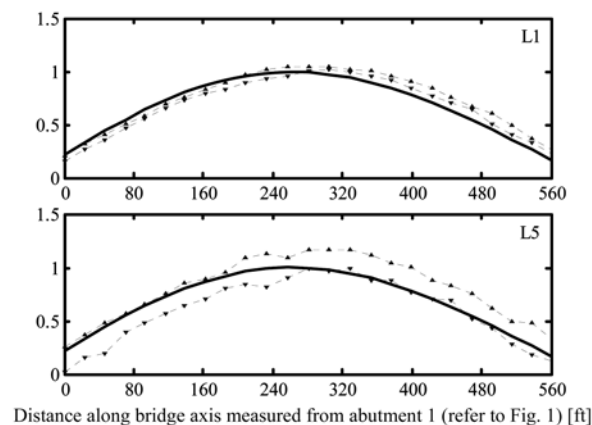


Fig. 5 Comparison of the first mode shape confidence bounds for S5 (dashed lines) and the damaged TRB system first mode shape at load stage 1 of pushover analysis

Table 2 Fractions of first mode shape components for TRB damaged system from pushover analysis displaying change outside confidence bounds of identified healthy mode

Load stage	Noise level L1					Noise level L5				
	S1	S2	S3	S4	S5	S1	S2	S3	S4	S5
1	3/3	6/7	7/7	12/13	22/25	1/3	5/7	5/7	7/13	4/25
2	2/3	5/7	6/7	11/13	13/25	0/3	0/7	2/7	3/13	2/25
3	3/3	7/7	7/7	13/13	25/25	3/3	7/7	7/7	13/13	24/25
4	3/3	7/7	7/7	13/13	25/25	3/3	7/7	7/7	13/13	24/25

data with lowest noise level L1 (Table 1) and sensor configuration S5 (Table 1), the change of the mode shape of TRB for stage 1 could be deemed statistically meaningful. However, if data with noise level L5 (also from S5 sensor configuration) is used for SI of the healthy system modal parameters, the change in the first mode shape for this early stage of damage, i.e. the yielding of the first column of TRB, is mostly within the confidence interval of the identified healthy parameters and therefore is statistically insignificant.

The fractions of first mode shape components that displayed statistically significant changes out of the confidence intervals of the SI results of the healthy system are given in Table 2 for different sensor configurations, all load stages and low noise level (L1) as well as high noise level (L5). These fractions of mode shape components are given with respect to the total number of mode shape components recorded on the bridge deck, Table 1. The importance of the noise level in the data used for identification is prominent in the first mode results as shown in Table 2. For load stages 1 and 2, the degree of noise is the primary factor in determining the number of mode shape components that can be used for HM, i.e. those outside the confidence bounds. Moreover, Table 2 shows that load stage 2 corresponding to

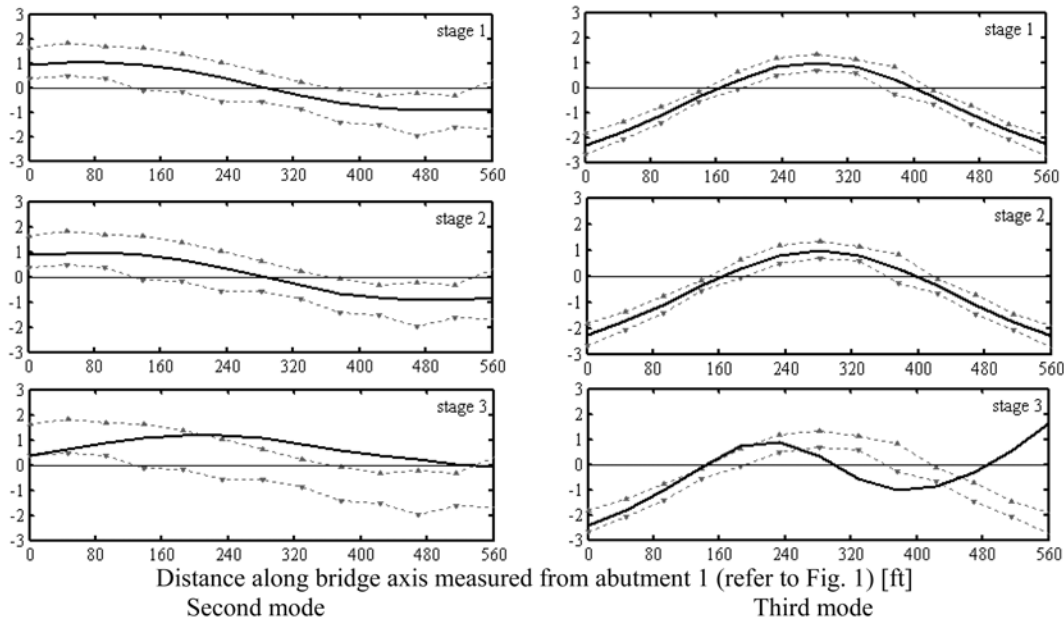


Fig. 6 Comparison of the higher mode shape confidence bounds using data from S5 sensor configuration with L5 noise level (dashed lines) and the damaged TRB system higher mode shapes

Table 3 Fractions of higher mode shape components for damaged TRB system from pushover analysis displaying change outside confidence bounds of identified healthy modes (noise level L5)

Load stage	Mode 2					Mode 3				
	S1	S2	S3	S4	S5	S1	S2	S3	S4	S5
1	0/3	0/7	0/7	0/13	0/25	0/3	0/7	0/7	0/13	0/25
2	0/3	0/7	2/7	3/13	2/25	0/3	0/7	0/7	0/13	0/25
3	2/3	3/7	3/7	4/13	3/25	1/3	2/7	4/7	5/13	17/25
4	1/3	4/7	4/7	6/13	9/25	2/3	4/7	5/7	6/13	20/25

higher damage level than load stage 1 is actually harder to detect based on mode shape information. This can be explained by considering the pattern of change in TRB modal parameters; the bridge mode shape with both columns in flexural yielding is very similar to the healthy mode shape. For the ultimate load stages, the first mode shape components are drastically different from those of the healthy system properties and it is not surprising that all corresponding mode shape quantities indicated change in the bridge.

The changes in the second and third mode shapes due to damage are not statistically significant for critical load stages 1 and 2 in the pushover analysis similar to the corresponding modal frequencies, Fig. 4. As shown in Fig. 6, only at high damage level due to the loss of the stiffness of the abutment for stage 3, changes in the second and third mode shapes become statistically significant. The insensitivity of the higher mode shapes to loss of stiffness in bridge columns and the high uncertainty in the estimation of these modal parameters render the adoption of these higher mode shapes unfeasible for HM of column members in a bridge system such as TRB. For the second and third mode shapes, the damage indicators for each mode shape, i.e. fractions of mode shape components displaying statistically significant change, are provided in Table 3. The changes in these mode shapes due to load stages 1 and 2 are clearly statistically insignificant. However, stages 3 and 4 displayed statistically significant changes. It is noted that the data noise level has no effect where even for level L1, nearly none of the identified components of the higher mode shapes can be utilized for detecting yielding damage in the columns of TRB.

3.3. HM based on additional damage cases of TRB components

Different cases of damage on TRB columns and abutments are considered and the sensitivity of the bridge modal parameters to these damage cases is investigated. The damage cases are simulated by reduction of the stiffness of individual components in the FE model, Table 4. The eigen solution of these damage cases is carried out to obtain the modal parameters, which represent an analogy for results that can be obtained using SI of aftershock data after major earthquakes. For the column elements, the Young's modulus of the elements composing the bases of the columns is reduced. Note that the height of the portion of the column with reduced Young's modulus, namely 17 ft \approx 18% of the column height, is 1.5 times the width of the column cross-section. The damage in abutments is simulated in the FE model by reducing the initial stiffness of the spring elements at the ends of the bridge deck, Fig. 1b, with the selected reduction factors. The twelve simulated damage cases, Table 4, are applied separately to the FE model. The reductions of the modal frequencies for the damage cases in Table 4 are presented in Fig. 7 from eigen solution of the damaged elastic FE model. For the first 6 cases, the first modal frequency is not very sensitive to selected levels of reduction ($\leq 75\%$) of the bridge column stiffness. Therefore, changes in first modal frequency due to these damage scenarios are not statistically significant for

Table 4 Selected simulated damage cases of structural components for TRB FE model

Damage case	Selected structural component	Reduction in elastic modulus
1		25%
2	Column 1	50%
3		75%
4		25%
5	Column 2	50%
6		75%
7		50%
8	Abutment 1	70%
9		90%
10		50%
11	Abutment 2	70%
12		90%

healthy system parameters obtained from noisy data (L5) using sensor configuration S4. Moreover, changes in the modal frequency for the first two cases of abutments 1 and 2 damages (cases 7, 8, 10, and 11) are not statistically significant. In general, the first modal frequency is insensitive to the selected damage cases (except for severe cases such as 9 and 12, Table 4) and therefore is not a good indicator of small to medium damage in TRB.

The second and third modal frequencies are determined to be very sensitive to changes in boundary conditions simulated by damage cases 7 to 12, Fig. 7. Therefore, these modal parameters can be effectively used to determine damage in bearings, abutments and seating arrangements of TRB. However, these

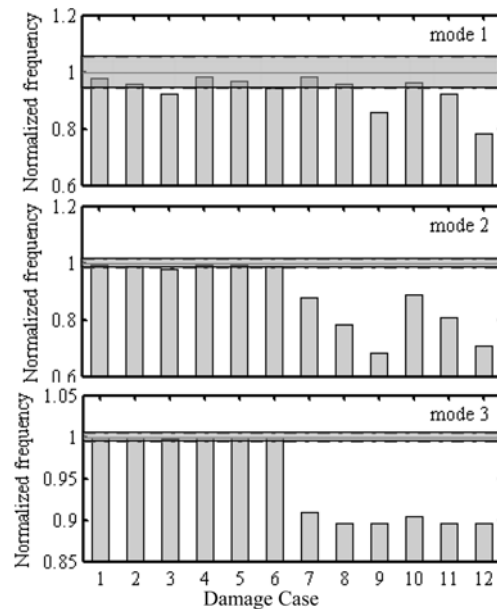


Fig. 7 Variation of normalized modal frequencies (with respect to the no-damage case) of the damaged TRB and confidence bounds of estimated healthy parameters (sensor configuration S4 and noise level L5)

Table 5 Fractions of mode shape components for different damage cases of TRB system displaying change outside the confidence bounds of identified healthy parameters (noise level L5)

Damage case	Mode 1					Mode 3				
	S1	S2	S3	S4	S5	S1	S2	S3	S4	S5
1	0/3	0/7	0/7	1/13	0/25	0/3	0/7	0/7	0/13	0/25
2	1/3	0/7	0/7	1/13	0/25	0/3	0/7	0/7	0/13	0/25
3	1/3	1/7	2/7	2/13	1/25	0/3	0/7	0/7	0/13	0/25
4	0/3	0/7	0/7	2/13	0/25	0/3	0/7	0/7	0/13	0/25
5	0/3	0/7	1/7	2/13	0/25	0/3	0/7	0/7	0/13	0/25
6	1/3	2/7	1/7	2/13	0/25	0/3	0/7	0/7	0/13	0/25
7	2/3	4/7	4/7	6/13	7/25	0/3	0/7	0/7	0/13	8/25
8	3/3	5/7	5/7	9/13	15/25	0/3	2/7	2/7	1/13	14/25
9	3/3	7/7	7/7	12/13	24/25	0/3	3/7	4/7	4/13	19/25
10	2/33	5/7	5/7	10/13	10/25	0/3	0/7	0/7	0/13	7/25
11	3/3	5/7	5/7	11/13	19/25	0/3	1/7	1/7	0/13	12/25
12	3/3	7/7	7/7	13/13	23/25	0/3	2/7	2/7	2/13	15/25

higher modal parameters are not sensitive to damage in the column flexural stiffness as they are not affected at all from reductions of column stiffness even for up to 75% reduction. The damage indicators for mode shape quantities, i.e. the fractions of mode shape components whose changes are statistically significant compared to the total number of mode shape components recorded on the bridge deck, are presented in Table 5 for all damage cases. From Table 5, the first mode shape clearly displays higher fractions of statistically significant changes with damage cases while the observed large confidence interval of the third mode shape precluded that. The second mode shape results are not included in Table 5 since it is found that for all damage cases its changes are within the confidence interval for this mode from the healthy system and accordingly its change is statistically insignificant.

In conclusion, among the considered modal parameters, the modal estimates that are most suitable for damage detection and HM include the first three modal frequencies and the first mode shape. Even with these limited estimates, due to the insensitivity of modal parameters to damage in bridge columns, the detection of column damage is only possible for extreme reduction in column stiffness of about 75%. While the second mode shape is not usable for HM purposes of TRB due to uncertainty in the estimation, the tight confidence interval for the third mode shape using sensor configuration S5 renders this third mode shape eligible for use in HM to detect damage in the abutments. However, this is an exceptional case as changes in the third mode shape are statistically insignificant for all damage scenarios using S1 for the other sensor configurations, i.e. S1 to S4.

4. Utilization of strong motion data and aftershock recordings

The damage in TRB is simulated in an idealized way in the previous section using either pushover analysis or equivalent reduction in material properties. However, this type of FE model manipulation can realistically model cases of simple loading or deterioration associated with brittle or sudden failure of components, i.e. loss of load carrying capacity of a member, failure in bearings, connections, etc. On the other hand, the design principles of structures in seismic regions rely on ductility of the members,

e.g. bridge bents, to survive damaging earthquakes. In this section, use of SI models to determine modal parameters of a bridge damaged by a large earthquake is investigated. To this end, the TRB FE model used in the previous section is subjected to a damaging earthquake and an aftershock for investigating the change in modal parameters. Recursive analysis on a Multi-Input/Single-Output (MISO) or Multi-Input/Multi-Output (MIMO) systems can be performed to capture the system changes due to a damaging seismic event (Arici and Mosalam 2006). However, recursive analysis is generally computationally demanding and is not pursued here. Instead, the aftershock following a damaging event is used for SI of TRB to obtain damaged system modal parameters. The feasibility of obtaining simple linear state space SI models from aftershock data is investigated. This way, aftershocks, frequently recorded after damaging events, can be used to monitor the structural integrity of a bridge. The reference modal parameters of the bridge signifying the system healthy state can be obtained from prior smaller earthquake events or from pre-shocks to a major event.

4.1. Nonlinear transient analysis

Two ground motions are selected to simulate the effect of a damaging earthquake and an aftershock on TRB. The fault normal component of the Olive View recording for Northridge earthquake (1/17/1994, Fig. 8a) is used as the damaging event in the simulation whereas the free-field component of the 2/12/2000 event recorded on TRB, Fig. 8b, is used as the aftershock motion. The moment-curvature response of the bridge columns at the base sections is obtained using fiber element discretization of the cross-section in OpenSees with the as-built section dimensions and reinforcement detailing. This complex

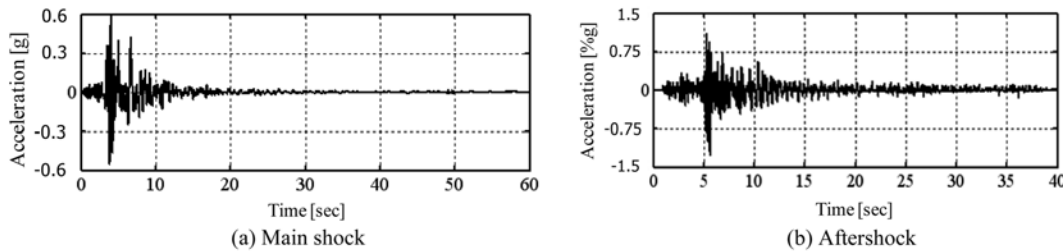


Fig. 8 Input ground motion time histories for transient analysis

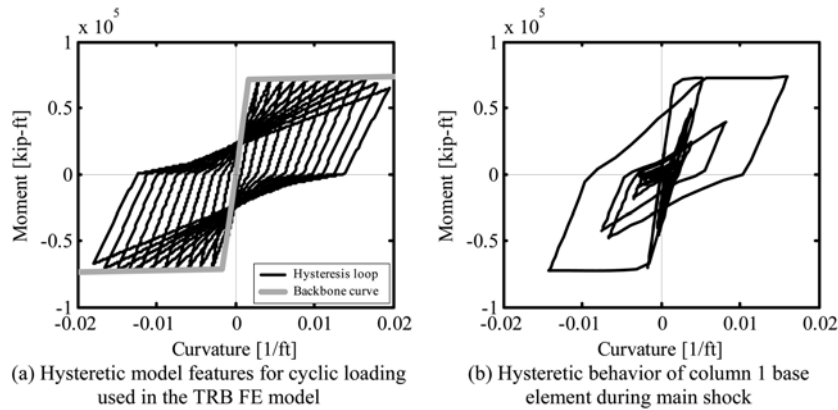


Fig. 9 Hysteretic model and response of the column bases for TRB FE model

moment curvature response is idealized as a bilinear relationship in a hysteretic model incorporating strength and stiffness degradation. Moreover, pinching is also considered in the hysteretic model. The response of the utilized section model for cyclic loading is shown in Fig. 9a. During the main shock, the bridge columns display severe nonlinear behavior as shown Fig. 9b. The transient analysis is conducted for the main shock and aftershock using OpenSees where Newmark method, $\beta=0.5$, $\gamma=0.5$, is used for numerical integration and the Newton-Raphson algorithm is used for the nonlinear solver (Mazzoni, *et al.* 2004). A free vibration period of no input ground motion is provided between the main shock and the aftershock. From this transient analysis, the decay of the first three modal frequencies is shown in Fig. 10a. These modal parameters are obtained using the eigen solution of the tangent stiffness matrix at each time step. Clearly, the stiffness of TRB rapidly deteriorated after the first big pulse at about second 4 of the main shock.

The effect of hysteretic nonlinear behavior on the identified modal frequencies is clearly observed after second 4 of the main shock in the form of two different envelopes of the varying instantaneous frequency. This behavior is caused by the difference in the tangent stiffness matrix of TRB before and after damaged elements reached yielding. Moreover, pinching is responsible for stiffness variation in the hysteretic loop of damaged elements. An average measure of TRB stiffness deterioration is obtained by temporal averaging of the instantaneous modal frequencies, $f_i^I(t)$, for the i^{th} mode of the system using,

$$f_i(t) = \left(\int_{t-T_w/2}^{t+T_w/2} f_i^I(\tau) d\tau \right) / T_w \tag{1}$$

where $T_w = 2$ sec is the selected window width for averaging the frequencies. Using this measure, the variation of the modal frequencies plotted in Fig. 10a is smoothed in Fig. 10b. From these smooth plots, reductions in modal frequencies continued during the aftershock event. However, the deterioration is less rapid compared to the main shock event. An Auto-Regressive eXogenous (ARX) model (Arici and

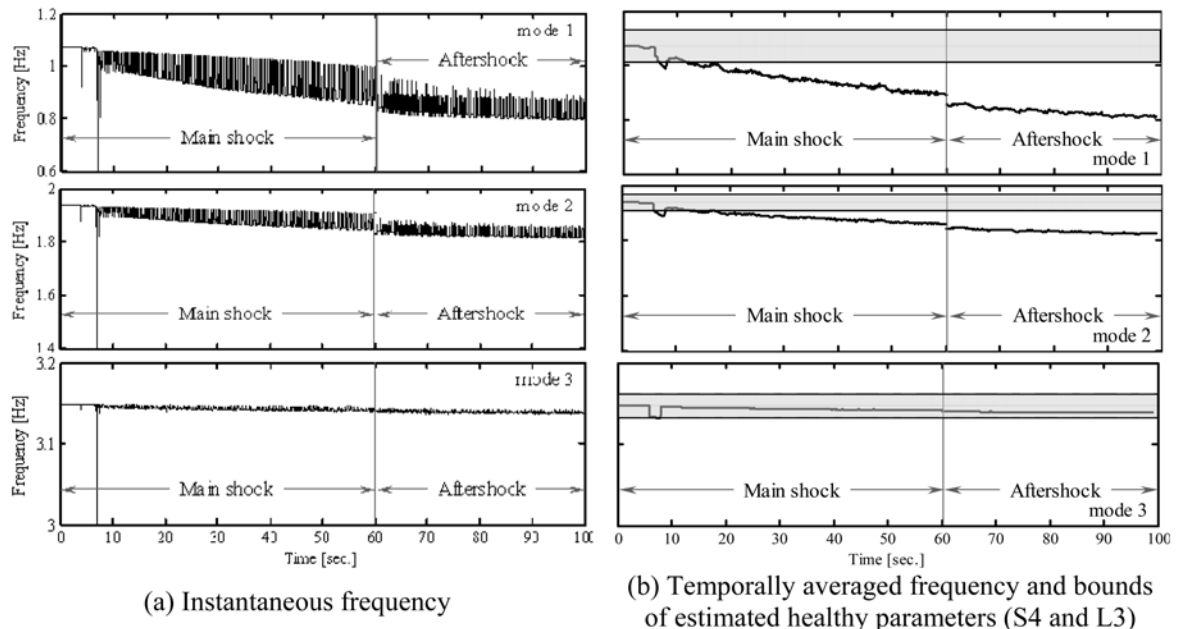


Fig. 10 Time variation of modal frequencies for main shock and aftershock transient analysis of TRB FE model

Mosalam 2003, 2006), forming an equivalent linear system for the bridge, is used in the next sub-section to model this complex behavior and obtain the modal parameters of the TRB system from the aftershock time history data.

4.2. Determination of modal parameters using aftershock recordings

The modal parameters of the TRB, including the modal frequencies and damping ratios are estimated in this sub-section using the aftershock strong motion data. For practicality, the time history data from the aftershock of the damaged TRB after application of the main shock is polluted with noise level L3 for S4 sensor configuration, Table 1. The modal frequencies and damping ratios estimated using the Observer Kalman filter Identification/Eigen Realization Algorithm with Direct Correlations (OKID-ERA-DC) (Arici and Mosalam 2005a, 2005b, 2006) from this polluted aftershock data are compared to the healthy system modal parameters in Table 6. The modal parameters of the healthy TRB system correspond to the elastic FE model.

The modal frequencies are reduced to some extent due to the effect of the main shock. According to Table 6, these changes are detected from the aftershock data. Moreover, the detected changes are close to those from the temporally averaged modal frequencies obtained using OpenSees, Fig. 10b. It is noted that because of the nonlinear nature of the TRB FE model, accurate modal information of the system could only be captured by linear models of high model reduction order, $p = 24$, (Arici and Mosalam 2006). Note that p determines the number of independent parameters of the observer Kalman ARX filter used in OKID-ERA-DC. In addition, the estimates are extremely noise dependent. Accordingly, filtering of high frequency content in data is crucial in obtaining accurate SI models of the TRB system. For the presented model, the mean simulation error (Arici and Mosalam 2006) for all the output components is 20.8%. Although adequate, this quality of fit shows that, for aftershock data, use of linear models is not straightforward. The mode shapes identified using the aftershock data is presented in Fig. 11 along with the SI estimates for the healthy bridge system. The change in the first mode shape is easily observed and this change is statistically significant for some of the modal components. However, the

Table 6 Comparison of healthy and damaged TRB modal parameters from aftershock data (S4 and L3)

Mode	Healthy TRB structure		Damaged TRB structure	
	f [Hz]	ζ [%]	f [Hz]	ζ [%]
1	1.07	5.34	0.84	9.36
2	1.94	5.16	1.78	7.22
3	3.14	6.30	3.11	2.72

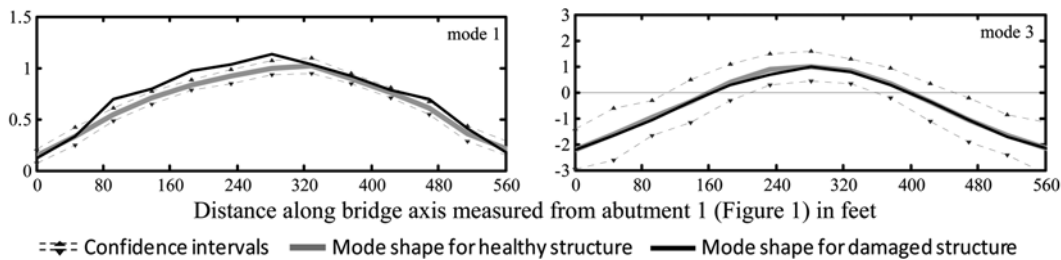


Fig. 11 Mode shapes for healthy and damaged TRB from aftershock data (S4 and L3)

third mode shape does not change in any statistically significant manner and clearly is not affected by the damage induced on the TRB by the main shock of the ground motion.

5. Conclusions

The sensitivity of the modal parameters of TRB to damage scenarios is investigated. The statistical significance of the modal property changes caused by damage is evaluated in light of the confidence bounds of the identified healthy modal parameters. Moreover, use of aftershock data for identification and HM of the damaged system is investigated. From the discussion, the following conclusions are inferred:

- The modal parameters of TRB are not sensitive to flexural damage simulated on the bridge columns. Only after significant yielding of the flexural steel in the columns and the accompanying drastic stiffness loss, the modal parameters display statistically significant changes.

- The use of only the first three modal frequencies and the first mode shape is feasible for further utilization of modal data in HM of TRB. Notably, even the first mode shape, due to its insensitivity to damage, is a partially effective damage detection tool for the TRB columns. However, the first mode shape is effective for monitoring changes in the boundary conditions. On the other hand, the second and third mode shapes obtained from strong motion data are ineffective for HM purposes of TRB.

- The limitations of the use of selected modal parameters for SI are discussed. In light of the large width of the confidence intervals of the estimated parameters and the general insensitivity of the modal parameters of TRB to moderate damage of the system, particularly those for the columns, these modal parameters can only be used for HM purposes for large degradations in the stiffness properties.

- For severe scenarios of damage induced on TRB, increasing the number of sensors on the system increases the number of mode shape components that display significant change compared to the confidence intervals of the healthy mode shapes. However, for less severe damage scenarios, including damage scenarios of TRB columns short of excessive yielding, increasing the number of sensors does not affect the number of statistically significant damage indicators obtained.

- Aftershock data is successfully used to obtain damaged modal parameters of TRB system. However, the reduction in modal frequencies due to damage accumulation on TRB required the use of high model reduction orders to obtain a representative linear SI model of the damaged system.

Acknowledgement

The study was partially funded by California Strong Motion Instrumentation Program (CSMIP) under contract 1098-714 with funding from the California Department of Conservation.

References

- ACI Committee 318-02 (2003), *Building Code Requirements for Structural Concrete and Commentary*, American Concrete Institute, Detroit.
- Arici, Y. and Mosalam, K.M. (2006), "Modal identification and health monitoring of instrumented bridges using seismic acceleration records", Technical Report, EERC 2006-2, Earthquake Engineering Research Center, University of California, Berkeley.

- Arici, Y. and Mosalam, K.M. (2003), "System identification of instrumented bridge systems", *Earthq. Eng. Struct. D.*, **32**(7), 999-1020.
- Arici, Y. and Mosalam, K.M. (2005a), "Statistical significance of modal parameters of bridge systems identified from strong motion data", *Earthq. Eng. Struct. D.*, **34**(10), 1323-1341.
- Arici, Y. and Mosalam, K.M. (2005b), "Modal identification of bridge systems using state-space methods", *J. Struct. Control Health Monit.*, **12**(3-4), 381-404.
- Beck, J.L. (1983), "System identification applied to strong motion records from structures", *Earthquake Ground Motion and Its Effect on Structure*, AMD, **53**, 109-133.
- Cakmak, A.S., Rodriguez-Gomez, S. and DiPasquale, E. (1991), "Seismic damage assessment for reinforced concrete structures", *Proc. of the 5th Int. Conf. on Soil Dynamics and Earthquake Engineering*, Germany, Sept. **23-26**, 515-544.
- De Witte, F.C. (2003), *DIANA User's Manual: Release 8.1.*, TNO DIANA Bv.
- DiPasquale, E. and Cakmak, A.S. (1990), "Seismic damage assessment using linear models", *Soil Dyn. Earthq. Eng.*, **9**(4), 194-215.
- Farrar, C. and Jauregui, D. (1996), "Damage detection algorithms applied to experimental and numerical modal data from the I-40 bridge", Technical Report, LA-13074-MS, Los Alamos.
- Goel, R.K. and Chopra, A.K. (1995), "Seismic response study of the Hwy 101/Painter street overpass near Eureka using strong motion records", Data Utilization Report CSMIP/95-01, CSMIP.
- Loh, C.H., Chen, I.H. and Lin, C.Y. (1998), "System identification of frames under earthquake loading", *Asia-Pacific Workshop on Seismic Design and Retrofit of Structures*, Taipei.
- Mander, J.B., Priestley, M.J.N. and Park, R. (1988), "Theoretical stress-strain model for confined concrete", *J. Struct. Eng. ASCE*, **114**(8), 1804-1826.
- Maroney, B.H. and Chai, Y.H. (1994), "Bridge abutment stiffness and strength under earthquake loadings", *Proc. 2nd Int. Workshop on Seismic Design & Retrofitting of R.C. Bridges*, New Zealand.
- Mau, S.T. and Revadigar, S. (1994), "Detecting structural damage from building seismic records", *Proc. 5th U.S. National Conf. on Earthquake Engineering*, EERI, Oakland, California, **2**, 331-340.
- Mazzoni, S., McKenna, F., Scott, M.H. and Fenves, G.L. (2004), *OpenSees User's Manual*, Pacific Earthquake Engineering Center, University of California, Berkeley, <http://opensees.berkeley.edu>.
- Safak, E. (1999), "Wave-propagation formulation of seismic response of multistory buildings", *J. Struct. Eng. ASCE*, **125**(4), 426-437.
- Wood, M.G. (1992), "Damage analysis of bridge structures using vibrational techniques", Ph.D. Dissertation, Aston University, UK.